AIAA JOURNAL
Vol. 31, No. 6, June 1993

Comparison of Eight Variations of a Higher-Order Theory for Cylindrical Shells

R. A. Smith* and A. N. Palazotto†
Air Force Institute of Technology, Wright-Patterson Air Force Base, Ohio 45433

Eight variations of a geometrically nonlinear higher-order transverse shear deformation (HTSD) theory were developed for composite shells. Three attributes were varied to produce the eight variations. These attributes included: 1) the order of the thickness expansions used to approximate the shell shape factors, 2) the order of the assumed linear displacement field, and 3) the nonlinearity of transverse shear strain. Several cylindrical shell problems were investigated using a finite element code with a 36-degree-of-freedom cylindrical shell element. MACSYMA, a symbolic manipulation code, was used to formulate the element independent stiffness arrays for each variation of the theory. When all nonlinear strain displacement terms for transverse shear were included for thin shallow isotropic cylindrical shells, the theory predicted a more flexible response during collapse. Higher-order thickness expansions had negligible effect on results. For deep shells nonlinearity was limited to in-plane strain-displacement relations. This quasinonlinear HTSD theory produced a more flexible response during collapse when the order of approximation of shell shape factor terms was increased.

Introduction

THE goal of this research was to develop a nonlinear higher-order transverse shear deformation (HTSD) theory with more exact higher-order thickness expansions than used by previous researchers. In this case, the term nonlinear refers to using the full nonlinear Green-Lagrange strain tensor representation for the transverse shear strain components and for the in-plane strain components. Transverse shear deformation theories that use nonlinear terms for in-plane strains, but only linear terms for transverse shear strains, are referred to, in this research, as quasinonlinear HTSD theories. Nonlinear transverse shear deformation theories have been published in Refs. 1 and 2, but for the most part have been limited to kinematic assumptions based on first-order polynomials in terms of the thickness coordinate.[3–5] These theories are generally called first-order transverse shear deformation (FTSD) theories. Similarly, most researchers have truncated geometric shell shape factor approximations at the first-order terms of the corresponding thickness expansions.[3–13]

Review of Related Literature

For many years, the well-known Kirchhoff-Love assumptions were used as a starting point for shell theory derivations. These assumptions included a state of plane stress and inextensible normals that remained straight and normal during deformation. Dennis developed a large displacement, moderately large rotation, finite element formulation for laminated composite shells with a quasinonlinear HTSD theory.[7] Extensive studies by Dennis and Palazotto[8–10] and others[11–14] have used this quasinonlinear HTSD shell theory. Singh et al.[3] used a FTSD theory with selected nonlinear terms included in the transverse strain components.[3] They found transverse shear to be a significant factor in determining buckling load. Although this FTSD formulation included nonlinear transverse shear strains, the authors did not specifically evaluate the effects of the nonlinear terms. Palmerio et al.[4,5] published two papers on a moderate rotation nonlinear FTSD theory for laminated anisotropic shells. They indicated that their theory had nonlinear transverse shear strain terms, due to in-plane displacements, which were not present in a von Karman-type theory. Interestingly, they had to eliminate nonlinear transverse shear terms to reduce an overstiff behavior of the theory for a laminated composite cylindrical shell with transverse load.

Theory

The basic assumptions of a two-dimensional shell theory tied to the concepts of a reference surface (the midsurface of the shell) and a local curvilinear coordinate system associated with this surface. If one uses a Lagrangian description of deformation, all variables are expressed in terms of conditions prior to deformation. In this system, the displacement vector can be written in terms of orthonormal base vectors $\bar{e}_i$ ($i = 1, 2, 3$). For the shell, the Lame parameters A_α ($\alpha = 1, 2$) describe the two-dimensional relationship between the orthogonal surface base vectors a_α and their orthonormal counterparts $\bar{e}_\alpha$. The shell shape factors h_i ($i = 1, 2, 3$) describe the three-dimensional relationship between the orthogonal base vectors g_i of the three-dimensional orthogonal curvilinear coordinate system y_i and their orthonormal counterparts $\bar{e}_i$. For an orthogonal curvilinear coordinate system based on the lines of principal curvature of a shell, the shape factors are

$$h_1 = A_1(1 - y_3/R_1)$$
$$h_2 = A_2(1 - y_3/R_2) \tag{1}$$
$$h_3 = 1$$

where

$$A_1 = \left(\frac{\partial \boldsymbol{r}}{\partial \theta_1} \cdot \frac{\partial \boldsymbol{r}}{\partial \theta_1}\right)^{1/2}, \quad A_2 = \left(\frac{\partial \boldsymbol{r}}{\partial \theta_2} \cdot \frac{\partial \boldsymbol{r}}{\partial \theta_2}\right)^{1/2} \tag{2}$$

Thus, for the convenient case of a cylindrical shell, shown in Fig. 1, with radius $R_2 = R$ and local coordinates $\theta_1 = x$, $\theta_2 = s$, and z, described in an orthogonal space with global coordinates $y_1 = x$, $y_2 = s$ and $y_3 = z$, the position vector r (y_1, y_2, y_3) is given by

$$\boldsymbol{r} = x\boldsymbol{e}_1 + s\boldsymbol{e}_2 + z\boldsymbol{e}_3 \tag{3}$$

and the Lame parameters reduce to $A_1 = A_2 = 1$. Figure 1 also shows the 36-degree-of-freedom shell element used throughout this work.

Presented as Paper 92-2229 at the AIAA/ASME/ASCE/AHS 33rd Structures, Structural Dynamics, and Materials Conference, Dallas, TX, April 13–15, 1992; received April 17, 1992; revision received Oct. 29, 1992; accepted for publication Nov. 2, 1992. This work is declared a work of the U.S. Government and is not subject to copyright protection in the United States.

*Former Graduate Student; currently, Chief, Flight Vehicles Branch, Weapons Flight Mechanics Division, Armament Directorate, Wright Laboratory, Eglin Air Force Base, FL 32542. Senior Member AIAA.

†Professor, Aeronautics and Astronautics Department. Associate Fellow AIAA.

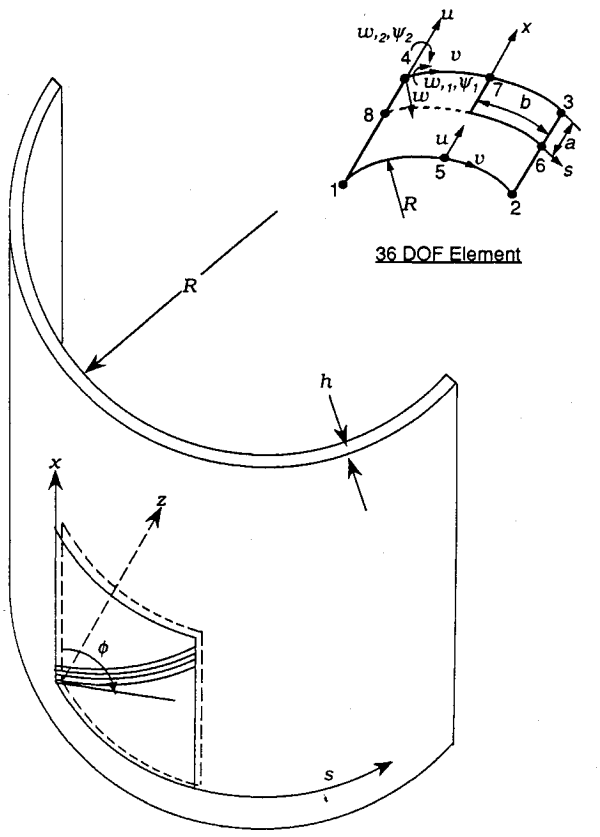

Fig. 1 Cylindrical shell domain for derivation of HTSD theory.

For this research, the macromechanical behavior of a composite lamina was assumed sufficient provided stresses were small enough to assure no material failure occurs. Thus, the material of each lamina was treated as a homogeneous anisotropic material. More specifically, the material was assumed to be transversely isotropic. This means the material has properties which are symmetric about two material axes. For a thin flat structural member, such as a plate, a state of plane stress is often assumed where σ_{13}, σ_{23}, and σ_{33} are all assumed to be equal to zero. In this research, however, the effects of transverse shear deformation were considered. Thus, σ_{13} and σ_{23} were not assumed to be zero. The direct normal stress σ_{33}, however, was still assumed to be zero. This assumption was necessary to reduce the three-dimensional problem to a two-dimensional problem. The direct transverse normal strain was assumed to be given by

$$\varepsilon_{33} = -\frac{C_{13}}{C_{33}}\varepsilon_{11} - \frac{C_{23}}{C_{33}}\varepsilon_{22} \tag{4}$$

where the C_{ij} are functions of material properties and ply layup.

There are several ways to include transverse shear deformation. Transverse shear effects can be included using an FTSD theory. In this case, material lines originally normal to the midsurface are allowed to deviate from the normal to the shell midsurface. These lines remain straight and inextensible. Since the angle of deviation is constant, the displacement field varies linearly through the thickness of the shell. The constant angle also implies transverse shear strain is constant and, thus, is not zero at the upper and lower surface of the shell. This inconsistent distribution results in a stiff model of the structure. This stiffening effect, called shear locking, becomes more pronounced as the shell thickness approaches zero. The HTSD theory allows the normal to rotate and warp. The HTSD theory for a flat plate produced a parabolic distribution of shear strain. This distribution matched the exact distribution of shear strain for the linear infinitesimal case. The results for curved shells, however, are different because of the curvature of the shell. These differences, due to curvature, were a primary concern of this research.

For a shell, the FTSD theory is given by the following displacement field:

$$u_1 = u(1 - y_3/R_1) + \psi_1 y_3$$
$$u_2 = v(1 - y_3/R_2) + \psi_2 y_3 \tag{5}$$

where the five degrees of freedom u, v, w, ψ_1, and ψ_2 are functions of the inplane curvilinear coordinates (y_1, y_2). The displacement field of a third-order linear transverse shear deformation theory is given by the following equations:

$$u_1 = u\left(1 - \frac{y_3}{R_1}\right) + \psi_1 y_3 - \frac{4}{3h^2}\left(\frac{\partial w}{\partial y_1} + \psi_1\right) y_3^3$$
$$u_2 = v\left(1 - \frac{y_3}{R_2}\right) + \psi_2 y_3 - \frac{4}{3h^2}\left(\frac{\partial w}{\partial y_2} + \psi_2\right) y_3^3 \tag{6}$$
$$u_3 = w$$

This third-order displacement field has two additional degrees of freedom not present in the first-order theory. These two degrees of freedom are the derivatives of transverse displacement w. These derivatives are, in the context of finite elements, independent degrees of freedom that represent the slope of the elastic curve. Thus, the third-order theory allows the slope of the elastic curve to deviate from the bending angles. This deviation is directly related to the transverse shear strains of the structure.

The third-order linear transverse shear deformation theory for a shell is suitable for many problems of practical interest. However, two approximations of this theory required further examination to assess their effects on the accuracy of this theory. Specific problems of interest were ones in which rotations and curvature within the element become very large. The first approximation in question was the neglect of some higher order terms in the thickness expansions of displacement field and the shell shape factor functions. For a shell, the third-order kinematics of the linear HTSD theory do not give zero linear transverse shear strains at the upper and lower surface unless the shell is flat or some small terms of the transverse shear strains are ignored. The curvature of the shell is important, because the shell shape factors distort the distribution of strain through the thickness of the shell, causing the distribution to be cubic rather than parabolic, as shown in Fig. 2. Thus, the order of approximation of the shell shape factors affects the accuracy of the strain distributions. The second approximation in question was the neglect of nonlinear transverse shear strain terms. The quasi-nonlinear HTSD theory ignores all nonlinear terms of both ε_{23} and ε_{13}. This linear restriction on ε_{23} and ε_{13} is not necessary physically, but satisfying the zero strain boundary conditions of the full nonlinear expressions is not a trivial problem.

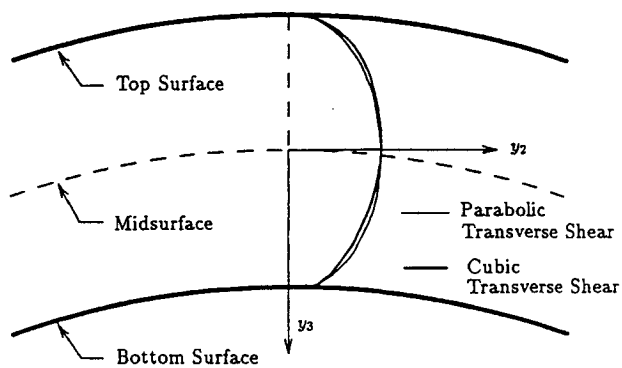

Fig. 2 Parabolic and cubic transverse shear strain distributions for a curved shell.

Table 1 Definition of elemental codes for variations of theory

Code name	Displacement assumption order	Shape factor approximation order	Transverse shear strains	Code length,[a] lines
C000	Cubic	Linear	Linear	13,866
C003	Cubic	Linear	Nonlinear	23,176
C020	Cubic	Quadratic	Linear	24,254
C023	Cubic	Quadratic	Nonlinear	39,322
C100	Quartic	Linear	Linear	29,626
C103	Quartic	Linear	Nonlinear	51,637
C120	Quartic	Quadratic	Linear	30,777
C123	Quartic	Quadratic	Nonlinear	67,618

[a]Code length is equal to the number of lines required to evaluate the K, N_1 and N_2 stiffness matrices using MACSYMA.

Table 2 Comparison of flat plate[a] displacement results for variations of geometrically nonlinear HTSD theory with linear and nonlinear transverse shear strain displacement

Total load, psi	7500	15,000	22,500	30,000	37,500
C000	0.4454	0.7982	1.076	1.308	1.513
C020	0.4454	0.7982	1.076	1.308	1.513
C100	0.4454	0.7982	1.076	1.308	1.513
C120	0.4454	0.7982	1.076	1.308	1.513
C003	0.4457	0.8001	1.081	1.317	1.527
C023	0.4457	0.8001	1.081	1.317	1.527
C103	0.4457	0.8001	1.081	1.317	1.527
C123	0.4457	0.8001	1.081	1.317	1.527

[a]Analyzed by discretizing one quadrant into a 4×4 mesh of uniform elements. Boundary conditions are: $x = 0$: $v = w_{,2} = \psi_2 = 0$ (symmetry); $s = 0$: $u = w_{,1} = \psi_1 = 0$ (symmetry); $x = \pm a/2$: $v = w = \psi_2 = 0$ (simple); $s = b/2$: $u = w = \psi_1 = 0$ (simple); $a = b = 8$ in.; $h = 1.6$ in.; $E_1 = 60\times10^6$ psi; $E_2 = 1.5\times10^6$; $G_{23} = 0.75\times10^6$ psi; $G_{12} = G_{13} = 0.9\times10^6$ psi; $\nu_{12} = 0.25$

The kinematics of Eq. (6) were modified to yield exactly zero at the top and bottom surface of a curved shell by adding two correction factors to the last term as follows:

$$u_1 = u\left(1-\frac{y_3}{R_1}\right)+\psi_1 y_3+\left(\psi_1+\frac{\partial w}{\partial y_1}\right)\times\left[-\frac{y_3^2}{R_1}+ky_3^3-\underline{\frac{k}{R_1}y_3^4}\right]$$

$$u_2 = v\left(1-\frac{y_3}{R_2}\right)+\psi_2 y_3+\left(\psi_2+\frac{\partial w}{\partial y_2}\right)\times\left[-\frac{y_3^2}{R_2}+ky_3^3-\underline{\frac{k}{R_2}y_3^4}\right] \quad (7)$$

$$u_3 = w$$

where $k = -4/(3h^2)$ and the underlined terms were the new terms added to Eqs. (6). These kinematics gave zero linear transverse shear strains at the upper and lower surfaces of a curved shell. The additional terms of Eqs. (7) also vanished for a flat plate, since each term was divided by radius of curvature. Likewise, for a right circular cylinder, with radius $R_2 = R$ and $R_1 = \infty$, the first equation of Eq. (7) reduced to the corresponding flat plate expression, since R_1 was infinite. The comparison of results from the incomplete cubic kinematics of Eqs. (6) and results from the complete quartic kinematics of Eqs. (7) was a major aspect of this research. As stated earlier, the cubic displacement field of Eqs. (6) was the same as used by other authors. The complete quartic, however, was a unique displacement field not derivable from those of other authors. Thus, this quartic displacement field was an exact solution for the linear traction free boundary conditions of a quasinonlinear HTSD theory for shells. This research compared the effects of cubic and quartic assumptions for the displacement field.

The nonlinear transverse shear boundary conditions are not as easily solved as the linear version of these conditions. The general fourth order kinematic assumptions, when substituted into the full nonlinear Green-Lagrange strain-displacement relations for ε_{13} and ε_{23}, gave two coupled nonlinear partial differential equations that were seventh-order in the thickness coordinate. This equation for ε_{13} is shown next.

$$\begin{aligned}\varepsilon_{13} = {} & \psi_1 + w_{,1} - cvv_{,1} + u_{,1}\psi_1 + v_{,1}\psi_2 + (2\phi_1 + 2\phi_1 u_{,1} \\ & + 2\phi_2 u_{,1} + c^2 uu_{,1} + \psi_{1,1}\psi_1 - cu\psi_{2,1} - cu_{,1}\psi_2 + \psi_{2,1}\psi_2)\, y_3 \\ & + (3\gamma_1 + 3\gamma_1 u_{,1} + 3\gamma_2 u_{,1} - 2\phi_2 cu_{,1} - cu\phi_{2,1} + 2\phi_1\psi_{1,1} \\ & + \phi_{1,1}\psi_1 + 2\phi_2\psi_{2,1} + \phi_{2,1}\psi_2)\, y_3^2 + (4\theta_1 + 4\theta_1 u_{,1} + 4\theta_2 u_{,1}) \\ & - 3\gamma_2 cu_{,1} - cu\gamma_{2,1} + 2\phi_1\phi_{1,1} + 2\phi_2\phi_{2,1} + 3\gamma_1\psi_{1,1} + \gamma_{1,1}\psi_1 \\ & + 3\gamma_2\psi_{2,1} + \gamma_{2,1}\psi_2)\, y_3^3 - (4\theta_2 cu_{,1} + 2\phi_1\gamma_{1,1} + 2\phi_2\gamma_{2,1} \\ & + 3\gamma_1\phi_{1,1} + 3\gamma_2\phi_{2,1} + 4\theta_1\psi_{1,1} + 4\theta_2\psi_{2,1} + \psi_1\theta_{1,1} - cu\theta_{2,1} \\ & + \psi_2\theta_{2,1})\, y_3^4 + (3\gamma_1\gamma_{1,1} + 3\gamma_2\gamma_{2,1} + 4\theta_1\phi_{1,1} + 4\theta_2\phi_{2,1} \\ & + 2\phi_1\theta_{1,1} + 2\phi_2\theta_{2,1})\, y_3^5 + (4\theta_1\gamma_{1,1} + 4\theta_2\gamma_{2,1} + 3\gamma_1\theta_{1,1} \\ & + 3\gamma_2\theta_{2,1})\, y_3^6 + (4\theta_1\theta_{1,1} + 4\theta_2\theta_{2,1})\, y_3^7 \end{aligned} \quad (8)$$

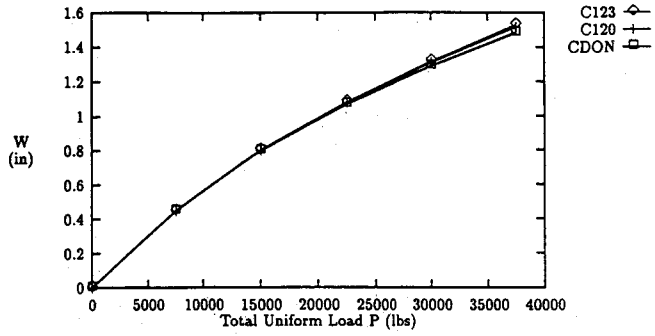

Fig. 3 Comparison of flat plate displacement results for variations of geometrically nonlinear HTSD theory with linear and nonlinear transverse shear strain displacement.

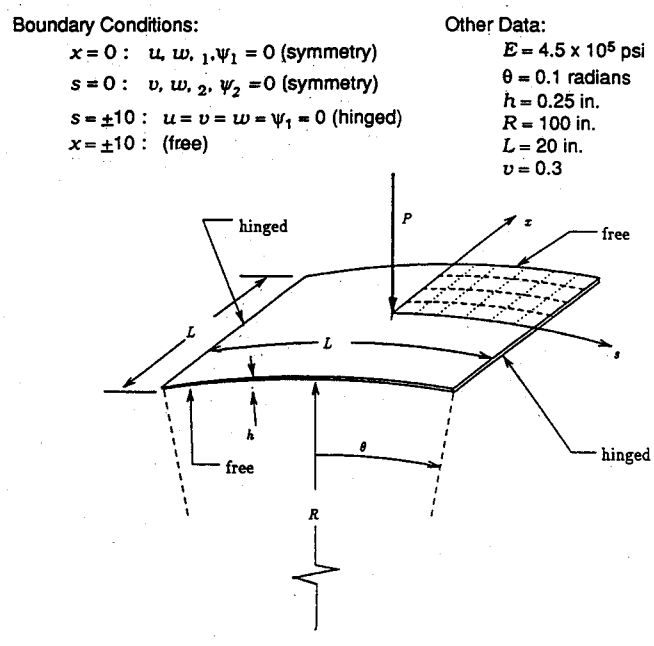

Fig. 4 Hinged-free point loaded isotropic cylindrical shell.

Table 3 Predicted transverse point load (lb) for center transverse displacement of a 1/4-in.-thick hinged-free isotropic shell

Disp., in.[a]	CDON	C000	C020	C100	C120	C003	C023	C103	C123
0.1	50.6	50.6	50.6	50.6	50.6	50.6	50.6	50.6	50.6
0.2	84.2	84.2	84.2	84.2	84.2	84.2	84.2	84.2	84.2
0.3	107.7	107.7	107.7	107.7	107.7	107.7	107.7	107.7	107.7
0.4	125.0	124.6	124.6	124.6	124.6	124.9	124.9	124.9	124.9
0.5	133.0	132.4	132.4	132.4	132.4	133.0	133.0	133.0	133.0
0.6	111.2	109.6	109.6	109.6	109.6	111.1	111.1	111.1	111.1
0.7	−86.6	−86.6	−86.6	−86.6	−86.6	−79.5	−79.5	−79.5	−79.5
0.8	−72.0	−71.5	−71.5	−71.5	−71.5	−66.3	−66.3	−66.3	−66.3
0.9	−40.3	−39.6	−39.6	−39.6	−39.6	−33.9	−33.9	−33.9	−33.9
1.0	13.9	14.7	14.7	14.7	14.7	22.2	50.6	22.2	22.2

[a]Displacement.

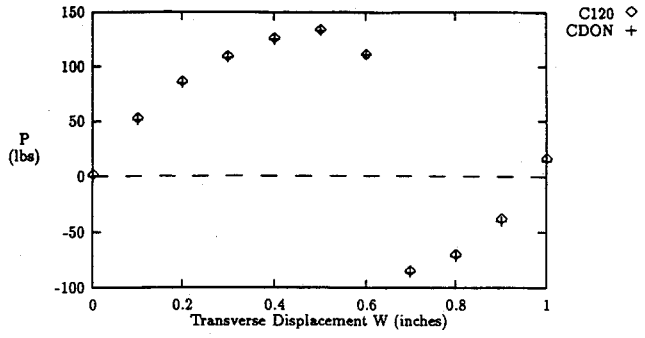

Fig. 5 Predicted transverse point load vs center transverse displacement for transversely loaded 1/4-in.-thick shell; CDON and C120 theories.

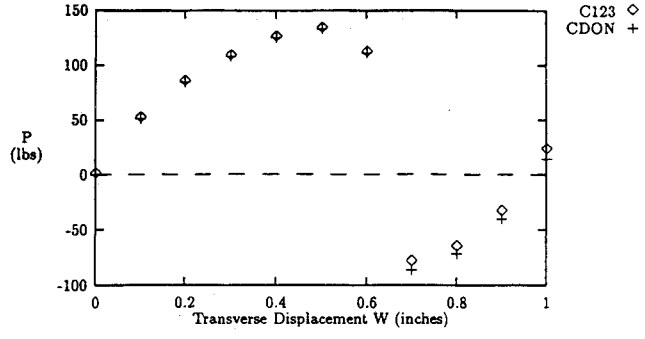

Fig. 6 Predicted transverse point load vs center transverse displacement for transversely loaded 1/4-in.-thick shell; CDON and C123.

where ϕ_i, γ_i, and θ_i were undetermined functions of the in-plane coordinates defined only on the midsurface of the shell. To solve the two equations for all of the unknown functions (there are six unknowns), one must evaluate the two equations at $y_3 = \pm h/2$ and set each resulting equation equal to zero. This is required to satisfy the zero traction boundary condition on the surfaces of the shell. Solving four coupled nonlinear partial differential with six unknowns was beyond the scope of this research project. Although other authors have proposed the use of nonlinear transverse shear strain-displacement relations with linear kinematics, none have done so within the context of a HTSD theory.

The authors' approach to including nonlinear transverse shear terms in the theory included several assumptions beyond those of the quasinonlinear HTSD theory. First, the authors were primarily interested in problems involving large rotations and curvature changes for laminated shells. Thus, the displacement field of the new theory should reduce to the displacement field of the linear HTSD theory for problems with smaller rotations or smaller curvatures. The kinematic assumptions of Eqs. (7) reduce to the kinematics of the linear HTSD theories for small curvature problems. Second, nonlinear kinematic assumptions were not used to satisfy the nonlinear boundary conditions for ε_{13} and ε_{23}. The incorporation of nonlinear kinematic terms and the corrective terms of Eqs. (7) was prohibitive. Thus, the authors chose to use the linear kinematics of Eqs. (7) with the full nonlinear transverse shear relations and an approximate approach to the nonlinear boundary conditions. This approximate approach assumed the nonlinear transverse shear strain should be zero at the upper and lower surfaces and that the strain energy of the nonlinear transverse shear strain terms was excessive. The authors achieved a slight reduction in transverse shear strain energy and forced the satisfaction of zero traction, at the shell's surfaces, by multiplying the nonlinear transverse strain terms by a parabolic function of the thickness coordinate. Other researchers have used similar functions to provide the parabolic transverse shear distribution of linear HTSD theory.[3–5] This research compared the effects of linear and nonlinear strain-displacement relations for the transverse shear strain components.

A third "attribute" was also considered in this research, and that was the order of the approximation of functions of the shell shape factors. These functions appear in one strain displacement relation as functions of the shape factors and their derivatives. For a cylindrical shell, these geometric functions depend only on the thickness coordinate. For a FTSD or HTSD theory, where displacements are expanded in terms of the thickness coordinate, these geometric functions are often expanded in terms of the thickness coordinate and arbitrarily truncated at a specific power of the thickness coordinate. This research compared the effects of linear and quadratic approximations for the shell shape factor functions appearing in the equations for strains.

The preceding discussion of theory dealt with the development of the displacement field assumptions, the strain-displacement relations, and the constitutive relations for laminated composite shells. The next phase in the research was the development and solution of the governing differential equations for shell problems. Since the authors were specifically interested in the nonlinear phenomena of large displacements and rotations, no analytical or linear solutions were desired. The finite element technique was used to obtain numerical solutions for cylindrical shells. The finite element equations were based on the total potential energy of the elastic body. Specifically, the principle of stationary potential energy was used where the first variation of potential energy of the system is set equal to zero. The potential energy expression was found by first examining the equilibrium state of the body. For a body with prescribed force on part of its surface and prescribed boundary conditions on the remaining part of the surface, the equations of equilibrium for an infinitesimal virtual displacement were developed in terms of the second Piola Kirchhoff stress tensor and the Green strain components expressed in the body's coordinate system. Assuming strains were small, then the stresses could be written in terms of the strains. For a laminated orthotropic material, the stress components could be written in terms of the reduced structural stiffness of the lamina. These quantities depended only on the thickness coordinate. Thus, they could be written in terms of an integral over the midsurface of the shell, with the integration in the thickness direction performed analytically.

The variation of total potential energy gave five coupled nonlinear partial differential equations that governed the equilibrium of the system. These expressions contained 18 displacement parameters: u, $u_{,1}$, $u_{,2}$, v, $v_{,1}$, $v_{,2}$, w, $w_{,1}$, $w_{,2}$, $w_{,11}$ $w_{,22}$, $w_{,12}$, ψ_1, $\psi_{1,1}$, $\psi_{1,2}$, ψ_2, $\psi_{2,1}$, and $\psi_{2,2}$. The parameters included the seven displacement parameters of Eqs. (7) and their derivatives. Since the equilibrium equations were nonlinear in terms of the displacement parameters, an incremental-iterative approach was used to solve a system of linearized equations which yields an equivalent solution. For simple theories, such as Donnell's theory or a linear FTSD theory where relatively few terms are included, the first variation of potential energy and its linearization can be explicitly developed, term by term. For more complete theories, such as a linear HTSD theory or the fully nonlinear theory, the potential energy expression has several hundred terms. Its first variation would include, perhaps, thousands of terms, and the subsequent linear equilibrium equations would be quite lengthy. Rajasekaran and Murray[15] developed a formal procedure for finite elements that defined the total potential energy, its first variation, and the linear incremental equilibrium equations in terms of three stiffness matrices. Specifically, the total potential energy was given by

$$\Pi_p = \{q\}^T\left[\frac{1}{2}[K] + \frac{1}{6}[N_1] + \frac{1}{12}[N_2]\right]\{q\} - \{q\}^T\{R\} \quad (9)$$

where

$\{q\}$ ≡ a column array of nodal displacement parameters

$\{R\}$ ≡ a column array of nodal loads

$[K]$ ≡ an array of constant stiffness coefficients

$[N_1]$ ≡ an array of nonlinear coefficients with each term dependent on one of the displacement parameters ($[N_1]$ is linear in terms of displacement)

$[N_2]$ ≡ an array of nonlinear coefficients with each term dependent on the product of two displacement parameters ($[N_2]$ is quadratic in terms of displacement)

The first variation of potential energy then was given by

$$\left[[k] + \frac{1}{2}[N_1] + \frac{1}{3}[N_2]\right]\{q\} - \{R\} = \{0\} \quad (10)$$

and the linear incremental equilibrium equation was given by

$$[[K] + [N_1] + [N_2]]\{\Delta q\} - \{\Delta R\} = \{0\} \quad (11)$$

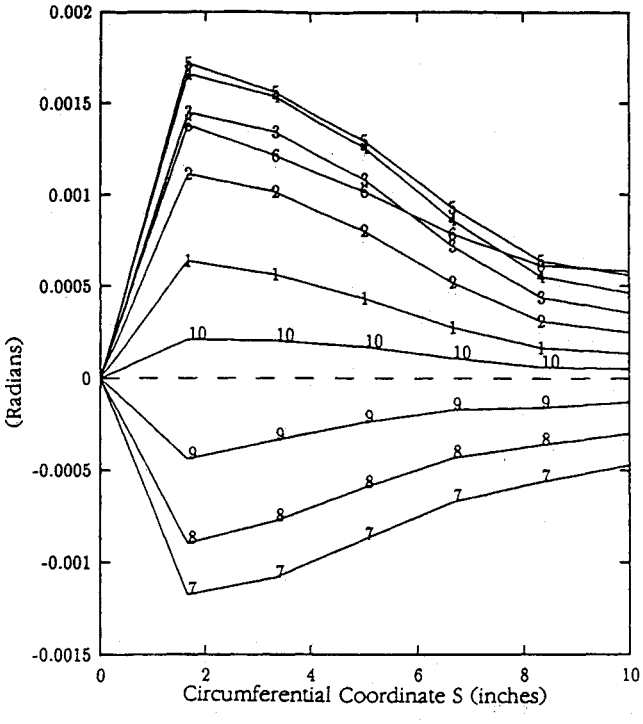

Fig. 7 Meridian values of $\psi_2 + w_{,2}$ for 10 increments (0.1 in. each of transverse displacement); CDON theory.

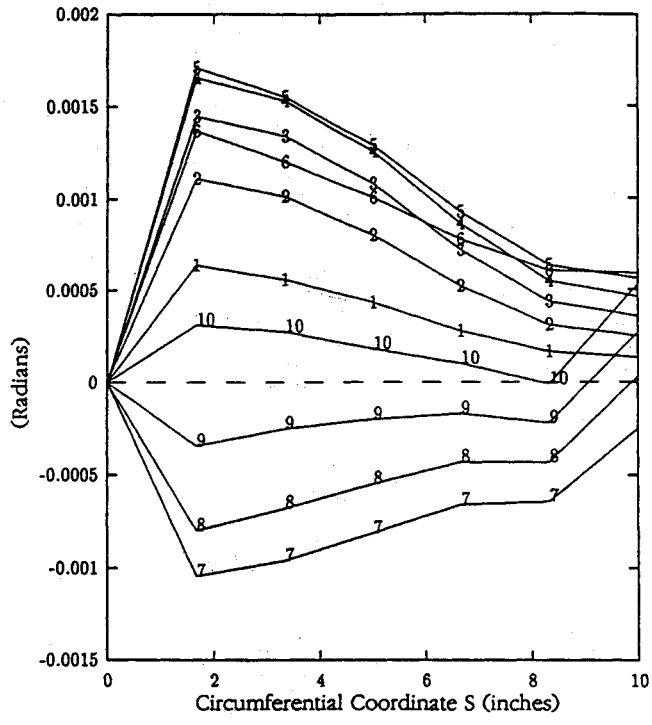

Fig. 8 Meridian values of $\psi_2 + w_{,2}$ for 10 increments (0.1 in. each of transverse displacement); C123 theory.

To insure that the formalism of Eqs. (9–11) held, the stiffness arrays $[K]$, $[N_1]$, and $[N_2]$ had to be derived in a specific fashion. This derivation is discussed in Ref. 14.

The two-dimensional integration of the finite element equations, in the plane of the finite element, was accomplished by numerical integration using Gaussian quadrature. Solution of the resulting equations was accomplished by an incremental-iterative technique commonly called the Newton-Raphson method. The parameters to be incremented were the elements of the array $\{q\}$, containing global degrees of freedom. A global criterion, written in terms of the norms of all displacement parameters, was used to determine convergence. The 36-degree-of-freedom element shown in Fig. 1 was described in Refs. 7–14 and the details of the element development will not be included herein.

Eight versions of the theory were produced for this research. Each of the versions were written as subroutines, called elemental codes, which were called by a main finite element program. The elemental codes calculate the elemental stiffness matrices. The theoretical attributes of the elemental codes are summarized in Table 1. The codes are identified by a symbol "GXYZ," defined as follows:

G = C for cylindrical, S for spherical, or A for arbitrary shell geometry. (Appendix A of Ref. 14 lists relations for arbitrary shells and Appendices B–E list relations for cylindrical shells. Complete relations for spherical shells were not generated for this research.)

$X = 0$ for the incomplete cubic u_2 displacement of Eqs. (6), or 1 for the complete quartic u_2 displacement of Eqs. (7).

$Y = 0$ for linear shell shape function approximations, or 2 for quadratic approximations.

$Z = 0$ for linear transverse shear strain displacement relations, or 3 for nonlinear relations.

CDON = the Donnell shell equations with through-the-thickness shear included using $X = 0, Y = 0$.

Results

Flat Quasi-Isotropic Panel with Uniform Transverse Pressure Load

A transversely loaded flat plate problem was used to test the MACSYMA generated elemental codes and the modified finite element program. The plate chosen was an 8-ply quasi-isotropic laminated square plate with simple boundary conditions along

each of its 16-in.-long sides. The plate was loaded with a uniform transverse pressure load. The plate thickness was 1.6 in., which is 1/10 of the edge length and should indicate transverse shear may be important. The four quasinonlinear HTSD codes (C000, C020, C100, and C120) produced identical results; see Table 2. This close agreement shows that the authors' theories correctly degenerate to flat plate solutions when curvature is not a factor in the problem. Similarly, the four nonlinear HTSD codes (C003, C023, C103, and C123) predict identical results. The fully nonlinear codes, however, predict a slightly greater transverse displacement than the quasinonlinear codes (as shown in Fig. 3).

Hinged-Free Isotropic Shell Panel, 0.25 in. Thick, with Transverse Point Load

The second problem investigated was a thin hinged-free isotropic cylindrical shell with transverse point load. The 1/4-in. thick shell is shown in Fig. 4. Geometric and material properties are also given for this problem in the same figure. Solutions were computed using a 4×6 mesh of elements to model one quadrant of the shell (six elements are in the circumferential direction). Table 3 shows the results of equilibrium load predictions, for increments of transverse displacement from 0.1 to 1.0 in., for the eight elemental codes and the modified-Donnell theory with transverse shear included (CDON). From this table one observes the quasinonlinear HTSD codes (C*XX*0) all produce the same results, and the nonlinear HTSD codes (C*XX*3) all produce the same results. The results of the CDON, C120, and C123 codes were selected for more detailed analysis because they represent the three variations with different results.

Figure 5 shows the equilibrium paths of transverse load vs center-point displacement for the 1/4-in. thick shell predicted by the CDON and C120 codes whereas Fig. 6 replaces C120 with C123. As in the flat plate case, the results for the quasinonlinear HTSD codes are all the same. In contrast, the nonlinear HTSD codes all show slightly greater flexibility (a smaller magnitude of load) during the collapse phase (from $w = 0.7$–0.9) than the quasinonlinear HTSD variants.

This result is interesting because this phase of the collapse is characterized by the most extreme displacements and rotations occurring in the problem. The inclusion of nonlinear transverse shear terms for this problem had a noticeable effect on load-displacement results. Figures 7 and 8 show values of the linear χ_4^0 transverse shear term $\psi_2 + w_{,2}$ for 10 increments for transverse displacement w for the CDON and C123 theories, respectively. Values plotted are the values of $\psi_2 + w_{,2}$, at nodes along the $x = 0$ line from the center of the panel ($s = 0$) out to the hinge line ($s = 10$). The labels 1,...,10 indicate the first through tenth increments of transverse displacement w. These results are virtually identical for increments 1–6, before the shell snaps through. After the shell snaps, however, the values of $\psi_2 + w_{,2}$ are about 20–25% less in magnitude over the majority of the panel, where $1 \le s \le 8$, for the C123 theory as compared to the CDON quasinonlinear theory. In Fig. 8, the value of $\psi_2 + w_{,2}$ is dramatically more positive at the hinge line ($s = 10$) during increments 7–10 for the C123 theory than for the CDON theory.

These figures show the values of only the linear term of the χ_4^0 term of the ε_{23} strain at the midsurface of the shell. For the nonlinear HTSD theory, the ε_{23} and ε_{13} strain components include many

Table 4 Comparison of maximum values of linear and nonlinear terms of χ_4^0 for the 1/4-in.-thick cylindrical shell (radius)

		Increment					
Code name	χ_4^0 term	1	5	7	8	9	10
CDON	$\psi_2+w_{,2}$	0.0006	0.0017	−0.0012	−0.0009	−0.0004	0.0002
C123	$\psi_2+w_{,2}$	0.0006	0.0017	−0.0010	−0.0007	−0.0003	0.0003
C123	$-w\psi_2/R_2$	0.0000	−0.0002	−0.0004	−0.0005	−0.0006	−0.0008
C123	$y_2+w_{,2}-wy_2/R_2$	0.0006	0.0015	−0.0014	−0.0012	−0.0009	−0.0005

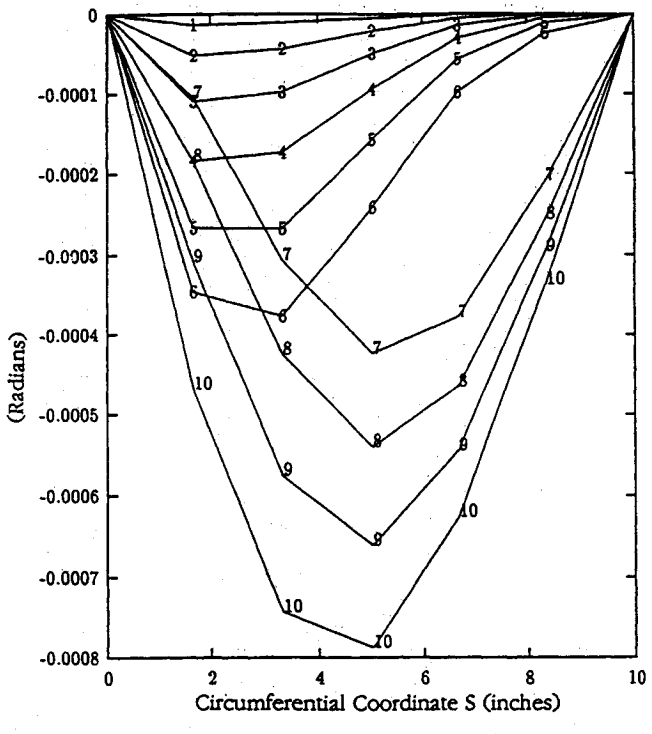

Fig. 9 Meridian values of $-w\psi_2/R_2$ for 10 increments (0.1 in. each of transverse displacement); C123 theory.

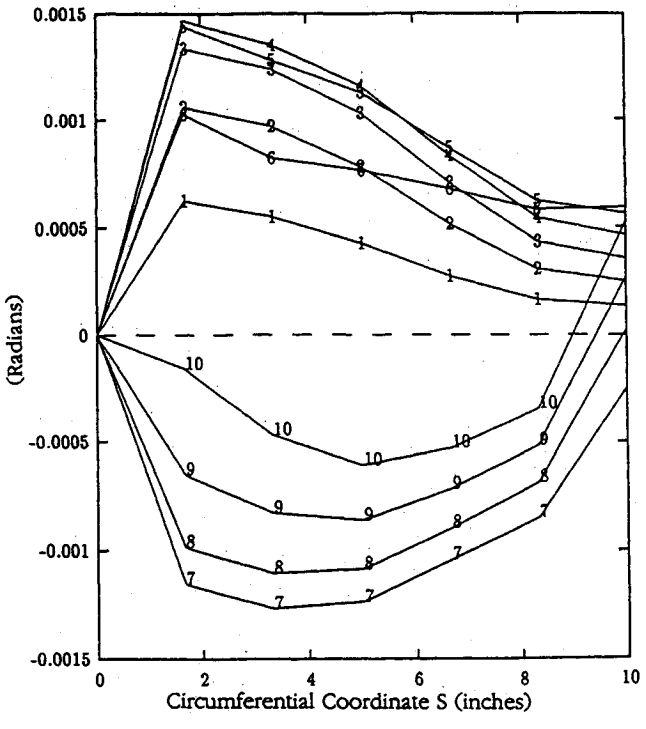

Fig. 10 Meridian values of $\psi_2 + w_{,2} - w\psi_2/R_2$ for 10 increments (0.1 in. each of transverse displacement); C123 theory.

Table 5 Transverse center-point load (lbs) predicted for prescribed transverse displacement of a 100-in.-radius hinged-free deep isotropic cylindrical arch

Disp., in.	CDON[a]	C000	C020	C100	C120	C120†
4	621.24	640.6	640.0	640.6	640.0	632.5
8	893.66	914.8	911.6	914.8	911.6	899.1
12	1028.2	1018.6	1010.2	1018.6	1010.2	993.9
16	1088.3	929.5	914.0	929.5	914.0	978.7
20	1100.5	898.7	872.7	898.7	872.7	879.3
24	1078.4	775.3	728.7	775.3	728.7	705.2
28	1029.5	548.5	471.9	548.5	471.9	440.3
32	958.56	52.9	−232.3	52.0	−232.1	[c]

[a]Values taken from Ref. 7, p. 259. [b]Computed with a 1 × 48 element mesh. [c]Datum point not computed.

more nonlinear terms. These terms are shown for the C003, C023, C103, and C123 theories in Appendices B–E of Ref. 14 as χ^p_{4NL} and χ^p_{5NL} . The distribution of shear strain is significantly affected by including the nonlinear transverse shear terms. Figure 9 shows the largest nonlinear term of the χ^0_4 term of the transverse shear strain component for the C123 theory. This term $-w\psi_2/R_2$ and the linear term $\psi_2 + w_{,2}$ are the predominant terms of the χ^0_4 strain component. Table 4 shows a comparison of these terms for the three theories. From Table 4, for increment 5 when the largest magnitude of $\psi_2 + w_{,2}$ occurs, the maximum values of $\psi_2 + w_{,2}$ and $-w\psi_2/R_2$ are 0.0017 and −0.0002, respectively. Thus, the largest nonlinear term of C123 is less than 20% of the linear term. With each increment from 7 to 9 (after the shell has snapped through), the nonlinear term becomes more significant compared with the linear terms. This nonlinear term, although it is of comparable magnitude with the linear terms, creates a softening effect. It effectively increases the magnitude of the transverse shear strain over a large area of the shell's midsurface.

Figure 10 shows the value of $\psi_2 + w_{,2} - w\psi_2/R_2$ for the C123 theory. Comparing this figure with Figs. 7 and 8 reveals the significant difference in the transverse shear terms for the nonlinear theory, as compared to the quasinonlinear HTSD theories. This difference is large enough to affect the strain energy of the shell and subsequently results in slightly different equilibrium values of the nodal displacements for the C123 theory as compared to the CDON or C120 theories. At increment 10, when the largest magnitude of $-w\psi_2/R_2$ occurs, the magnitude of this nonlinear term exceeds that of the linear terms by some 800%. Thus, the beneficial effect of transverse shear has been totally obliterated by the nonlinear terms of this formulation. Palmerio et al.[5] reported an overstiff response for similar shells when nonlinear transverse shear was included in their formulation.

Deep Isotropic Cylindrical Arch with Transverse Point Load

Deep circular arches can be used to demonstrate a theory's ability to predict large displacements and rotations. Many variations of transversely loaded deep arch problems have been reported in the literature. The problem chosen here is a 100-in. radius arch with a 1-in. square cross section and an opening angle of 106 deg. The arch configuration is shown in Fig. 11 along with geometric and material data. The equilibrium solutions for this problem were computed using all eight elemental codes with 1 × 16 and 1 × 48 element meshes to represent one quadrant of the arch. Data from the quasinonlinear theories are shown in Table 5. Figure 12 shows load vs crown displacement values predicted by the C100 and C120 theories. Both the C000 and C100 theories predicted the same results. The C100 theory, however, does not give any more flexible results than the C000 theory despite the more exact u_2 displacement assumptions. The C020 and C120 theories both predict a more flexible response after collapse than the C000 and C100 theories.

Discussion

This research revealed several unique findings related to the limitations of a nonlinear HTSD shell theory employing higher-order thickness expansions and linear kinematic assumptions. Similar studies with first-order transverse shear deformation theories were recently accomplished, but no studies of this nature have been accomplished for a third- or higher-order transverse shear deformation theory. The ratio of thickness to wave length of curvature (distance between counter-flexure points of the deformed midsurface) and the ratio of transverse displacement to depth of the shell were found to be important factors in predicting the applicability of the nonlinear HTSD theory. If these ratios were negligible, nonlinear transverse shear strain terms had no impact on predicted response. If these ratios were small (on the order of 10^{-3}–10^{-1}), the incorporation of nonlinear HTSD theory produced a more flexible response. A shallow 1/4-in.-thick hinged-free isotropic shell panel exhibited this more flexible response with nonlinear strain-displacement terms in the transverse shear strain formulation.

Koiter[16] showed that typical shell theory assumptions resulted in transverse shear strains that were of the order h/L times the bending or direct strain components. For his work, strain and stress were directly related by the constitutive relations for linear elastic isotropic materials. Provided one assures the nonlinear transverse shear terms of the nonlinear HTSD theory do not result in transverse shear stresses exceeding h/L times the bending or direct stresses, this theory can be used for the prediction of nonlinear HTSD responses of curved shells.

Another objective of this research was to determine the effect of using higher-order thickness expansions for the displacement field assumptions and for the geometric shell shape factor approximations. Similar studies with transverse shear deformation theories were recently accomplished, but no studies of this nature have been accomplished for a fully nonlinear higher-order transverse shear deformation theory. The use of the complete quartic displacement assumption made no noticeable difference in static equilibrium load displacement results, as compared to the incomplete third-order HTSD kinematic assumptions. The authors believe the higher-order kinematic assumption would be important for shells with larger ratios of thickness to radii of curvature. Practical problems of the type investigated by the authors, however, can be accurately and efficiently solved with incomplete cubic kinematic assumptions.

The use of quadratic approximations for the shell geometric shape factor functions provided a more flexible response prediction for the deep circular arch during the collapse phase. However,

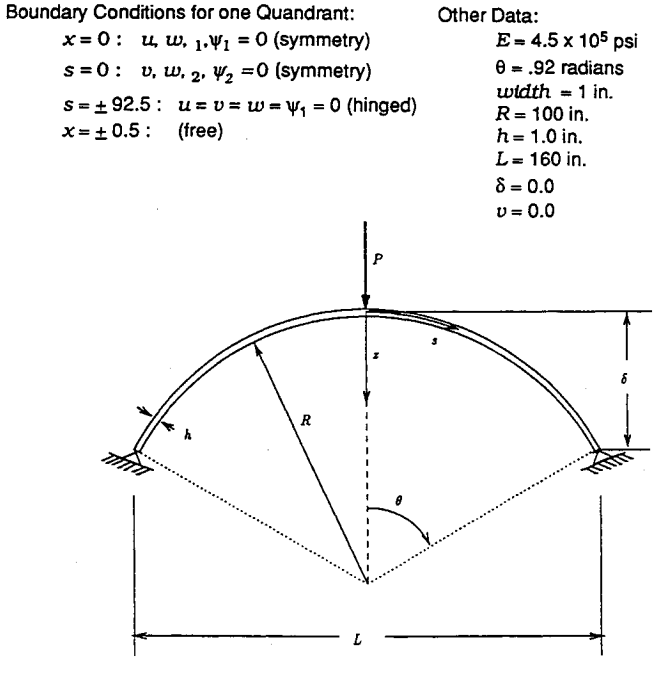

Fig. 11 Hinged point loaded isotropic cylindrical arch.

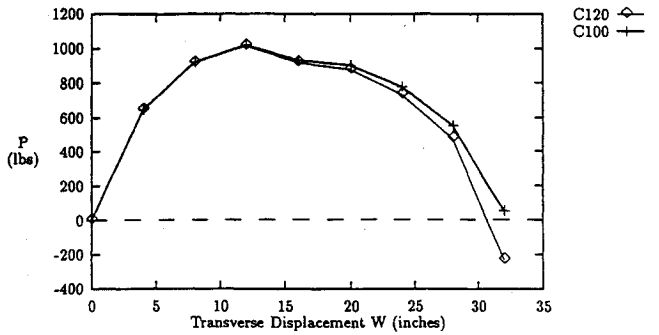

Fig. 12 Deep arch crown displacement vs load; C100 and C120 theories.

for the deep shell problem investigated, the ratio of h/R was equal to 1/100, thus, the effect of the higher-order shape factor approximations was not apparent until the deformation was significant. The deep arch required displacements of at least $R/4$ before the higher-order effect was recognizable. For the shallow shell panels analyzed, the quadratic shape factor approximations gave results identical to the linear shape factor approximations. The quadratic shape factor approximations, like the quartic displacement, significantly increased the number of lines of Fortran code required. Thus, the authors believe that quasinonlinear HTSD theories based on the assumption that $h^2/R^2 << 1$ are sufficiently accurate and economical for practical engineering analyses.

Conclusions

In summary, including higher-order thickness expansions in a quasinonlinear HTSD theory resulted in a more flexible response prediction for deep shell problems during the collapse phase for the problems considered. Similarly, the nonlinear HTSD theory provided a more flexible response prediction for shallow shell problems during the collapse phase. The incorporation of these theoretical characteristics required a significant increase in the amount of Fortran code with a proportional increase in the computational memory and time required for problem solution. The simplest nonlinear HTSD theory, developed for this research, incorporated incomplete third-order kinematics and a linear approximation of the shell geometric shape factor functions. This theory resulted in Fortran code about twice the length of the comparable quasinonlinear HTSD variant. Further investigations could be accomplished with this version of the theory, in lieu of the most complete nonlinear theory used for this research.

References

[1]Librescu, L., "Elastostatic and Kinetics of Anisotropic and Heterogeneous Shell-Type Structures," Noordhoff, Chap. IV, 1975, pp. 457–492.

[2]Librescu, L., "Refined Geometrically Nonlinear Theories of Anisotropic Laminated Shells," *Quarterly of Applied Mathematics,* Vol. 45, April 1987, pp. 1–22.

[3]Singh, G., Rao, S. Y. V. K., and Iyengsr, N. G. R., "Buckling of Thick Layered Composite Plates under In-Plane Moment Loading," *Composite Structures,* Vol. 13, 1989, pp. 35–48.

[4]Palmerio, A. F., Reddy, J. N., and Schmidt, R., "On a Moderate Rotation Theory of Laminated Anisotropic Shells—Part 1. Theory," *International Journal of Non-Linear Mechanics,* Vol. 25, No. 6, 1990, pp. 687–700.

[5]Palmerio, A. F., Reddy, J. N., and Schmidt, R., "On a Moderate Rotation Theory of Laminated Anisotropic Shells—Part 2. Finite-Element Analysis," *International Journal of Non-Linear Mechanics,* Vol. 25, No. 6, 1990, pp. 701–714.

[6]Kant, T., and Menon, M. P., "Higher-Order Theories for Composite and Sandwich Cylindrical Shells with C° Finite Element," *Computers and Structures,* Vol. 33, No. 5, 1989, pp. 1191–1204.

[7]Dennis, S. T., "Large Displacement and Rotational Formulation for Laminated Cylindrical Shells including Parabolic Transverse Shear," Ph.D. Dissertation, School of Engineering, Air Force Inst. of Technology (AU), AFIT/DS/ENY/88-1, Wright-Patterson AFB, OH, 1988.

[8]Dennis, S. T., and Palazotto, A. N., "Transverse Shear Deformation in Orthotropic Cylindrical Pressure Vessels Using a Higher-Order Shear Theory," *AIAA Journal,* Vol. 27, No. 10, 1989, pp. 1082–1088.

[9]Dennis, S. T., and Palazotto, A. N., "Static Response of a Cylindrical Composite Panel with Cutouts Using a Geometrically Nonlinear Theory," *AIAA Journal,* Vol. 28, No. 6, 1989, pp. 1082–1088.

[10]Dennis, S. T., and Palazotto, A. N., "Large Displacement and Rotational Formulation for Laminated Shells Including Parabolic Transverse Shear," *International Journal of Non-Linear Mechanics,* Vol. 25, No. 1, 1990, pp. 67–85.

[11]Tsai, C.-T. and Palazotto, A. N., "A Modified Riks Approach to Composite Shell Snapping Using a High-Order Shear Deformation Theory," *Computers & Structures,* Vol. 35, No. 3, 1990, pp. 221–226.

[12]Tsai, C.-T., and Palazotto, A. N., "Large-Rotation Snap-Through Buckling in Laminated Cylindrical Panels," *Finite Elements in Analysis and Design,* Vol. 9, 1990, pp. 65–75.

[13]Palazotto, A. N., and Dennis, S. T., *Nonlinear Analysis of Shell Structures,* AIAA Education Series, edited by J. S. Przemieniecki, AIAA, Washington, DC, 1992.

[14]Smith, R. A., "Higher-Order Thickness Expansions for Cylindrical Shells," Ph.D. Dissertation, School of Engineering, Air Force Inst. of Technology (AU), AFIT/DS/ENY/91-1, Wright-Patterson AFB, OH, Sept. 1991.

[15]Rajasekaran, S., and Murray, D. W., "Incremental Finite Element Matrices," *Journal of the Structures Division ASCE,* Vol. ST12, Dec. 1973, pp. 2423–2437.

[16]Koiter, W. T., "A Consistent First Approximation in the General Theory of Thin Elastic Shells," *The Theory of Thin Elastic Shells,* North-Holland, Amsterdam, 1960, pp. 12–33.